Temperature Influence on Lanthanoids(III) Hydration from Molecular Dynamics Simulations

Magali Duvail[a], Pierre Vitorge[a,b], Riccardo Spezia[a,*]

[a] *Laboratoire Analyse et Modélisation pour la Biologie et l'Environnement, UMR-CNRS 8587, Université d'Evry Val d'Essonne, Boulevard F. Mitterrand, 91025 Evry Cedex, France.*
[b] *CEA Saclay, Nuclear Energy Division, Physical Chemistry Department, SECR, LSRM, 91991 Gif Sur Yvette, France.*

Abstract

We studied temperature dependence of Lanthanoid(III) cations hydration by molecular dynamics simulations using explicit polarization. The main effect of the temperature (T) is to increase exchange frequencies between the two main stoichiometries and the proportions of the minor species. Activation energies for self-exchange reaction have a minimum in the middle of the series and the CN values of all Ln^{3+} ions tends to a limit 8.5 value at high temperature. Linear variations are found through the series for the Gibbs energies of water exchange reactions being of the origin of the coordination number sigmoidal variation across the series.

Keywords: Lanthanoid ions, Molecular Dynamics simulations, Temperature, Polarization

1. Introduction

Structure and dynamics at room temperature of lanthanoids(III), Ln^{3+}, cations were elucidated in last years by means of both theoretical [1, 2, 3, 4, 5, 6, 7, 8, 9, 10, 11, 12, 13, 14, 15] and experimental [16, 17, 18, 19, 20, 21] approaches. Recently, we have pointed out the importance of polarizability to correctly describe hydration structure and dynamics of the whole series [11, 12], confirming the previous findings of Helm, Merbach and co-workers [3, 4, 5]. Using classical molecular dynamics with explicit polarization (CLMD), we were able

*Corresponding author
Email address: riccardo.spezia@univ-evry.fr (Riccardo Spezia)

to have a very good agreement with experiments [22, 23] by . In particular, our model is able to gather key dynamical features that are at the basis of the understanding of hydration especially for atoms in the middle of the series [24]. Temperature dependence of exchange reactions can provide information on evolution across the series of Gibbs energies (and associated enthalpic and entropic contribution), as we have done previously for La^{3+} [25], but also on the activation energy for the same reaction. In particular it is of interest to make the link between thermodynamic properties and structural features.

Although temperature dependence of stabilities of aqueous hydroxides and complexes of f-block elements have been studied experimentally [26, 27, 28, 29], few temperature-dependence studies on Ln^{3+} hydration properties are reported in literature [30, 31]. In particular, few is known on the temperature influence on Ln^{3+} hydrations in the middle of the series where water self-exchange plays an important role [24]. In fact, while $Ln(H_2O)_9^{3+}$ and $Ln(H_2O)_8^{3+}$ stoichiometries are stable for elements at the beginning and at the end of the series respectively, in the middle of the series, an equilibrium between the two species is established via relatively fast interchangings [24, 19]. Therefore, for these latter Ln^{3+} ions temperature may induce changes in their structural and dynamical hydration properties since it should have a large effect on thermodynamic functions.

Free energy for self-exchange reactions are available from time-resolved laser fluorescence spectroscopy (TRLFS) [32] on Cm^{3+}, which is located in the middle of the actinoid series and thus often considered an analog of Gd^{3+}. In particular, they found that enthalpic and entropic contributions of the $Cm(H_2O)_8^{3+}/Cm(H_2O)_9^{3+}$ reaction of the same order of magnitude at room temperature assuming that temperature has a negligible effect on TRLFS of pure species. Similarly from ^{17}O NMR study it was found for Ce^{3+} that $\Delta_r H^0_{9,298}$ (-15 kJ mol^{-1}) and $298\Delta_r S^0_{9,298}$ (+7.6 kJ mol^{-1}) are of the same order of magnitude[31]. Note that such entropic and enthalpic contributions should almost cancel out in the middle of the series where the statistical coexistence of the two stoichiometries corresponds to CN = 8.5 [12, 24].

In the present work we report a molecular dynamics study of the temperature influence on hydration properties of some selected Ln^{3+}: Nd^{3+}, Eu^{3+}, Gd^{3+}, Tb^{3+}, Ho^{3+} and Lu^{3+}.

These Ln^{3+} cations have been chosen evenly in the series to have the best representation of the temperature effect on the structural and dynamical hydration properties through the series.

2. Methods

2.1. Simulation details

The total energy of our system is modelled as a sum of potential terms: (i) an electrostatic energy composed by a Coulomb and a polarization term – polarization was calculated following the Thole's induced dipole model [33] – (ii) a 12-6 Lennard-Jones potential describing the O-O interactions of polarizable TIP3P/P water molecules [11], and (iii) a *non electrostatic* Ln^{3+}-OH_2 interaction potential, represented by an exponential-6 Buckingham (Buck-6) potential. Details on the Hamiltonian employed and parametrization procedures are given in our previous works [11, 12].

Simulations of the hydrated Ln^{3+} ions (Ln^{3+} = Nd^{3+}, Eu^{3+}, Gd^{3+}, Tb^{3+}, Ho^{3+} and Lu^{3+}) have been carried out in the microcanonical *NVE* ensemble with our own developed classical molecular dynamics (CLMD) code MDVRY [34]. CLMD simulations were performed for one Ln^{3+} and 216 rigid TIP3P/P water molecules in a cubic box at the target temperature in the 277 - 623 K range. The size of the cubic box was adjusted to reproduce the density of pure liquid water at different temperatures (e.g. 1.000, 0.997, 0.9169 and 0.589 kg/dm^3 for 277, 298, 423 and 632 K respectively), as previously done for La^{3+} [35, 25]. Periodic boundary conditions were applied to the simulation box. Ewald summation was applied for computing long-range interactions [36] and an homogeneous background charge was applied to compensate for the ionic charge of the system. Simulations were performed using a Velocity-Verlet-Based Multiple Time Scale (MTS) with a 1 fs time step for positions and velocities and 5 fs for dipole dynamics. The system was equilibrated at the target temperature for 2 ps. Production runs were subsequently collected for 3 ns.

2.2. Thermodynamics analysis

The Gibbs energies changes of the

$$\mathrm{Ln(H_2O)_8^{3+} + H_2O \rightleftharpoons Ln(H_2O)_9^{3+}} \tag{1}$$

reactions were calculated from the corresponding equilibrium constant

$$\Delta_r G^0_{9,T} = -RT \ln(K^0_{9,T}) \tag{2}$$

with

$$K^0_{9,T} = \frac{n_9}{n_8} \tag{3}$$

where n_i is the number of configurations of the $\mathrm{Ln(H_2O)_i^{3+}}$ stoichiometry. We have employed the same approximations as in the previous study on La^{3+} [25]: (i) the ratio of the $\mathrm{Ln(H_2O)_9^{3+}}$ and $\mathrm{Ln(H_2O)_8^{3+}}$ activity coefficients was neglected and the activity of water (a_{H_2O}) was assumed to be 1 at any temperature (the usual origin for the water activity scales, a convention that ascribes all the temperature effects to the concentration ratios, and not to a_{H_2O}. For this reason we also use $\delta_{Ln}\Delta_r E$, the difference between $\Delta_r E$ values for different lanthanoids, where the H_2O terms cancel out typically for E = G, H or S). Further, (ii), the effects of the T and P variations are neglected during each simulation. Note that our simulations are in NVE ensemble but with these approximations all the properties will be the same as the ones calculated in NPT ensemble, e.g. free energy is Gibbs energy. $\Delta_r H^0_{9,T}$ was calculated from the van't Hoff approximation

$$R \ln(K^0_{9,T}) = R \ln(K^0_{9,T^0}) - \Delta_r H^0_{9,T^0}(\frac{1}{T} - \frac{1}{T^0}) \tag{4}$$

Our previous study on La^{3+} shows that this law is a reasonable approximation in our temperature range, confirming that the heat capacity ($\Delta_r C_{p,9}$) and the molar volume ($\Delta_r V_{m,9}$) changes can be neglected [25]. The entropy change was calculated from

$$\Delta_r G^0_{9,T} = \Delta_r H^0_{9,T} - T\Delta_r S^0_{9,T} \tag{5}$$

Considering only the main stoichiometries through the Ln series, *i.e.* nine and eight, the partial coordination number ($\widetilde{CN}$) is defined as follows:

$$\widetilde{CN} = 9 \times \frac{n_9}{N} + 8 \times \frac{n_8}{N} \tag{6}$$

where $N = n_8 + n_9$, it is almost the total number of configurations. Note that this defined $\widetilde{CN}$ is an approximation of CN that is obtained by integrating first peak of the Ln-O radial distribution functions, since $\widetilde{CN}$ takes into account only the two main stoichiometries, neglecting the minor ones. It is related to equilibrium constant, as defined in equation 3, such that it becomes:

$$\widetilde{CN} = 9 - \frac{1}{K^0_{9,298} + 1} \tag{7}$$

Within this approximation, the $\widetilde{CN}$ has a sigmoidal ($\mathcal{S}$) shape across the series, when approximately linear $\Delta_r G^0_{298,9}$ variation is observed as a function of the atomic number.

Activation energies E_a, corresponding to the $[Ln(H_2O)_8(H_2O)^{3+}]^{\#}$ transition state, have been calculated from mean residence times (MRTs) of water in the Ln^{3+} first hydration shells determined using the "direct method" [37, 11] as a function of temperature assuming the Arrhenius limit behaviour:

$$\frac{1}{MRT} = A \exp(-\frac{E_a}{RT}) \tag{8}$$

To have some insights on enthalpic ($\Delta H^{\ddagger}$) and entropic ($\Delta S^{\ddagger}$) effects on activation process, we also interpreted the associated rate constants with Eyring-Polanyi equation:

$$k_{ex} = \frac{k_B T}{h} \exp(\frac{\Delta S^{\ddagger}}{R}) \exp(-\frac{\Delta H^{\ddagger}}{RT}). \tag{9}$$

3. Results and discussions

3.1. Structural and dynamical properties

As shown in figure 1, temperature has not an important effect on the position of the peaks of Ln-O radial distribution functions (RDFs). Only second hydration shell peaks present a slight increase of the Ln-O maximum distance as the temperature increases, as already observed for La^{3+} [25]. At 623 K the first peak is wider and higher than for lower

temperatures, this being probably due the associated changes in density. Although temperature has no influence on the Ln-O distance of the first hydration shell, the first (and second) coordination number (CN) is effected by temperature. In particular, for light ions (here Nd^{3+} and Eu^{3+}) it decreases as temperature increases while for heavy ions (Ho^{3+} and Lu^{3+}) it increases as temperature increases (see Tab. 1). For all the studied Ln^{3+} ions, the CN is an average of different stoichiometries: from seven to eleven, depending on the Ln^{3+} ion and the temperature (Tab. 2), but 8 and 9 fold structures are always predominant. In most cases, increasing the temperature results in an increase of the minor stoichiometries, by typically less than 1 % at 275 K up to 10 % at 624 K for $Nd(H_2O)_8^{3+}$, and from 1 % at 276 K to 9 % at 619 K for $Lu(H_2O)_9^{3+}$ (Tab. 2). This effect is more important in the vicinity of the middle of the Ln series: a decrease of CN from 8.9 at 277 K to about 8.6 at 614 K is observed for Eu^{3+}, whereas for Ho^{3+}, the variations of CN are not monotonous, *i.e.* CN increase from 8.17 to 8.36 from 283 K to 419 K, while it decreases down again to 8.26 at 626 K (ser Tab. 1). Tb^{3+} has a different behavior. In fact, it has CN$\sim$8.5 already at low temperature, such that, since CN$\rightarrow$8.5 as T increases, temperature does not have a large effect on CN (while, as we will show later, it has on kinetics).

Changes in geometries – and therefore stoichiometries – as a function of temperature, through the Ln series, are also observed on the angular distribution functions (ADF). As already observed for La^{3+}, temperature has small effect on the O-Nd-O ADF peak positions: 70° and 137° that are the characteristic positions of the tricapped trigonal prism geometry [11] for the CN = 9 stoichiometry (Tab. 1). However, although the positions of the peaks do not vary as a function of temperature, an increase of the peak width is observed as shown in Fig. 2. The same observations are made for Eu^{3+}, *i.e.* quite small effect of temperature except on the peak width, even if changes of temperature lead to a decrease of its CN. On the other hand, ADFs of Ho^{3+} and Lu^{3+}, which are mainly coordinated to eight water molecules at room temperature, correspond to a mixture of three geometries: square antiprism (SAP), bicapped trigonal prism (BTP) and trigonal dodecahedron (DD), the ratio between these geometries depending on the temperature [12]. The 120° peak virtually disappears when increasing the temperature, especially in the case of Ho^{3+}. This can be explained

by the broadening of the 120° peak together with the increase of the base line between the two other –and bigger– peaks: by increasing the temperature, the distinction between the distorted (SAP, BTP and DD) geometries becomes even less clear. Note that in the case of Nd^{3+} and Eu^{3+} the peak at 120° is not present, even if their eight-fold stoichiometries proportions increase with temperature.

All these changes in the Ln^{3+} structural properties are associated with changes in the mean residence times (MRTs) of water molecules in their first hydration shells, and therefore on their dynamical properties. As already observed for La^{3+}, the increase of temperature leads to the decrease of the MRTs for all the systems studied, as reported in Tab. 1. This corresponds to easier water exchanges, that is a typical kinetic effect due to the increasing of temperature. Note that this dynamical effect is also observed on the RDFs (Fig. 1), since the increase of the peak width as a function of temperature is a direct consequence of the increasing number of water exchanges between the first and the second hydration shells. Although the MRTs are different through the Ln series at room temperature (from about 1 ns at the beginning and at the end of the series to hundreds of picoseconds for elements in the middle of the series), the MRTs reach a threshold value of about 30 - 40 ps at high temperature (624 K). At the beginning and at the end of the series, a single stoichiometry dominates in the whole temperature range studied: CN = 9 or 8 for the lightest (with larger ionic radii) or heaviest (with smaller ionic radii) Ln^{3+}, respectively. The less abundant stoichiometries, *i.e.* 8 and 10 at the beginning and 7 and 9 at the end of the series, are observed essentially during water exchanges. Increasing the temperature, the number of exchanges essentially increases and hence the proportion of the minor species increases. This is the main explanation of the observed CNs variations toward the 8.5 threshold value.

3.2. Thermodynamic interpretations

In Fig. 3 we show thermodynamic properties obtained across the series. We should remind that we interpret $\widetilde{CN}$, through Eq. 6, in terms of the corresponding chemical equilibrium of Reaction 1. Its equilibrium constant $K^0_{9,298}$ (Eq. 3), or equivalently the Gibbs energy change $\Delta_r G^0_{9,298}$, provides the thermodynamic interpretation (Eq. 2). Linear variation is

found for $\Delta_r G^0_{9,298}$ as a function of the atomic number Z (Fig. 3.b). Since the variations of r, the Shannon effective radius, or even $1/r$, are almost linear with Z, the variations of $\Delta_r G$ and $\Delta_r H$ are also linear. Such linear variations have been predicted by Miyakawa *et al.* based on an electrostatic model [30]. The linear variation of $\Delta_r G^0_{9,298}$(Z) provides the sigmoidal ($\mathcal{S}$ shape) variation of $\widetilde{CN}$ through the lanthanoid series (Eq. 7 and Fig. 3.d). Since the difference between the $\Delta_r G^0_{9,298}$ values for La^{3+} and Lu^{3+} is only 33.6 kJ mol^{-1}, we do not observe any sharp variation (or "break"), as structurally shown by EXAFS studies [20, 21]. Note that for Dy^{3+} we obtained $\Delta_r G^0_{9,298} \sim 0$ kJ mol^{-1}, which corresponds to CN = 8.5, in good agreement with our previous structural studies [12, 24].

Linear regression of the van't Hoff plots through the data points yields $\Delta_r H^0_{9,298}$ and $\Delta_r S^0_{9,298}$ values for this reaction. For all the studied Ln^{3+}, the entropic contribution ($T\Delta_r S^0_{9,298}$), is small and of the same order of magnitude of the error bars: from +3.9 for the beginning of the series to -0.3 kJ mol^{-1} for the end of the series, as shown in Tab. 3.

For this reason, the increase of $\Delta_r G^0_{9,298}$ across the lanthanoid series is essentially due to an enthalpic contribution as shown in figure 3. This can be interpreted as the decrease of the interaction strength of the ninth water molecule in the TTP structure with the decrease of the ionic radii across the series. The center of the sigmoid variation for CN from 9 to 8 (Fig. 3.d) corresponds to CN = 8.5, where $K^0_{9,T} = 1$ (Eq. 3) and $\Delta_r G^0_{9,T} = 0$ kJ mol^{-1} (Eq. 2). For the corresponding Ln^{3+} – between Tb^{3+} and Dy^{3+} – and for atoms in this region, the enthalpy and entropy of reaction contributions thus compensate.

$\Delta_r G^0_{9,298}$, $\Delta_r H^0_{9,298}$ and $\Delta_r S^0_{9,298}$ have been reported for Ce^{3+} [31, 30] and Cm^{3+} [27]. They are of the same order of magnitude as those we extracted from our MD simulations (Tab. 3). Note that the $\Delta_r G^0_{9,298}$ value published for Ce^{3+} assume CN = 8.8, while our previous simulations [12], in agreement with recent structural studies [21], and the quasi linear $\Delta_r G^0_{9,298}$ trend discussed above, reports higher values. It can be at the origin of the differences. The thermodynamic parameters we calculated for Eu^{3+} are close to the ones determined for actinoid Cm^{3+} by Lindqvist-Reis *et al.* [27], and especially for $\Delta_r G^0_{9,298}$. Therefore, Cm^{3+} can have almost the same behaviour as Eu^{3+} in aqueous solution, which is not totally surprising since they are located at almost the same place in the actinoid and

lanthanoid series, respectively.

The variation of the activation energy trough the Ln series follows the same trend as the one observed for the MRTs at room temperature, *i.e.*: it decreases first, reaching a minimum value for Tb^{3+} and then it increases, as shown in figure 4. Note that for atoms at the beginning of the series, i.e. from Nd^{3+} to Eu^{3+}, the activation energy corresponds to the barrier energy that one water molecule of the first hydration shell must overcome to go into the second shell, whereas at the end of the series, this energy corresponds to the barrier energy that one water molecule of the Ln^{3+} second hydration shell must overcome to go in the first one. Nevertheless, virtually the same values (about 15 - 16 kJ mol^{-1}) are obtained in both cases. The enthalpy-entropy decomposition obtained by Eyring-Polanyi equation (figure 4) shows that they both contribute to the speed up of self-exchange reaction in the middle of the series.

For lanthanoids being in the middle of the series, we observed a larger lability of water molecules between the first and the second hydration shell, as already observed studying water exchange frequency at room temperature [24]. Finally, we should note that the activation energy is smaller for La^{3+} than Nd^{3+}, due to the higher proportion of $La(H_2O)_{10}^{3+}$ observed compared to the other lanthanoid ions [25].

4. Conclusions

A detailed temperature study of Ln^{3+} hydration has been performed by means of CLMD with explicit polarization. The present work clearly highlights a temperature dependency on Ln^{3+} structural and dynamical properties. This dependency is also a function of the lanthanoid ion, and in particular on its position in the series. Indeed, although the Ln^{3+}-OH_2 distance in the first hydration shell does not vary much as a function of temperature, for all the studied lanthanoid ions, changes in the CN are observed, depending on the position of the lanthanoid in the series: a small difference is observed for ions at the beginning and at the end of the series – a slight decrease/increase for Nd^{3+} and Lu^{3+}, respectively – whereas it appears to be more temperature dependent in the vicinity of the middle of the series (with the obvious exception of ions, like Tb^{3+}, with already CN$\sim$8.5 at ambient

temperature). Note that EXAFS results on different cations by Seward and Fulton have shown slight changes in metal-water distances as a function of T [38, 39, 40].

Since entropy difference for the $Ln(H_2O)_8^{3+}/Ln(H_2O)_9^{3+}$ equilibrium is small and constant across the series, the decrease of $\Delta_r G^0_{9,298}$ is enthalpy driven. This result is consistent with the picture of lanthanoids as hard ions whose hydration number is essentially determined by ionic radius. Furthermore, the minor hydration numbers appear only during the water exchanges. CN tends toward the limit value of 8.5 when the frequency of these exchanges increases. This happens when increasing temperature or when approaching the size of the cation of the middle of the series. This is reflected by the lower activation energies found for lanthanoids located in the middle of the series.

Finally, our calculations of Eu^{3+} thermodynamic parameters are very close to those determined experimentally for Cm^{3+} [27], and structural data are similar to simulations done by Gagliardi and co-workers on Cm^{3+} [41]. These findings let us suppose that these two ions, located at almost the same place in their respective series, should have a very similar behaviour in aqueous solutions. This encourages us in extending our simple Ln^{3+} - OH_2 pair potentials to the actinoid series. Our research is currently going in that direction.

Acknowledgements

M.D. would like to thank Dr. P. Guilbaud for encouragement and support.

References

[1] W. Meier, P. Bopp, M. M. Probst, E. Spohr, J. L. Lin, J. Phys. Chem. 94 (1990) 4672–4682.

[2] L. Helm, F. Foglia, T. Kowall, A. E. Merbach, J. Phys.: Condens. Matter 6 (1994) A137–A140.

[3] T. Kowall, F. Foglia, L. Helm, A. E. Merbach, J. Phys. Chem. 99 (1995) 13078–13087.

[4] T. Kowall, F. Foglia, L. Helm, A. E. Merbach, J. Am. Chem. Soc. 117 (1995) 3790–3799.

[5] T. Kowall, F. Foglia, L. Helm, A. E. Merbach, Chem. Eur. J. 2 (1996) 285–294.

[6] F. M. Floris, A. Tani, J. Chem. Phys. 115 (2001) 4750–4765.

[7] C. Clavaguéra, R. Pollet, J. M. Soudan, V. Brenner, J. P. Dognon, J. Phys. Chem. B 109 (2005) 7614–7616.

[8] S. R. Hughes, T.-N. Nguyen, J. A. Capobianco, G. H. Peslherbe, Int. J. Mass Spectrom 241 (2005) 283–294.

[9] C. Clavaguéra, F. Calvo, J.-P. Dognon, J. Chem. Phys. 124 (2006) 074505.

[10] A. Ruas, P. Guilbaud, C. Auwer, C. Moulin, J.-P. Simonin, P. Turq, P. Moisy, J. Phys. Chem. A 110 (2006) 11770–11779.

[11] M. Duvail, M. Souaille, R. Spezia, T. Cartailler, P. Vitorge, J. Chem. Phys. 127 (2007) 034503.

[12] M. Duvail, P. Vitorge, R. Spezia, J. Chem. Phys. 130 (2009) 104501.

[13] A. Villa, B. Hess, H. Saint-Martin, J. Phys. Chem. B 113 (2009) 7270–7281.

[14] M. Duvail, A. Ruas, L. Venault, P. Moisy, P. Guilbaud, Inorg. Chem. 49 (2010) 519–530.

[15] J. J. Molina, M. Duvail, P. Guilbaud, J.-F. Dufrêche, J. Mol. Liq. 153 (2010) 107–111.

[16] C. Cossy, L. Helm, A. E. Merbach, Inorg. Chem. 27 (1988) 1973–1979.

[17] J. Näslund, P. Lindqvist-Reis, I. Persson, M. Sandström, Inorg. Chem. 39 (2000) 4006–4011.

[18] P. Allen, J. J. Bucher, D. K. Shuh, N. M. Edelstein, I. Craig, Inorg. Chem. 39 (2000) 595–601.

[19] L. Helm, A. E. Merbach, Chem. Rev. 105 (2005) 1923–1960.

[20] P. D'Angelo, S. De Panfilis, A. Filipponi, I. Persson, Chem. Eur. J. 14 (2008) 3045–3055.

[21] I. Persson, P. D'Angelo, S. D. Panfilis, M. Sandstrom, L. Eriksson, Chem. Eur. J. 14 (2008) 3056–3066.

[22] M. Duvail, P. D'Angelo, M.-P. Gaigeot, P. Vitorge, R. Spezia, Radiochim. Acta 97 (2009) 339–346.

[23] R. Spezia, M. Duvail, P. Vitorge, P. D'Angelo, J. Phys.: Conf. Ser. 190 (2009) 012056.

[24] M. Duvail, R. Spezia, P. Vitorge, ChemPhysChem. 9 (2008) 693–696.

[25] M. Duvail, R. Spezia, T. Cartailler, P. Vitorge, Chem. Phys. Lett. 448 (2007) 41–45.

[26] P. Zanonato, P. DiBernardo, A. Bismondo, G. Liu, X. Chen, L. Rao, J. Am. Chem. Soc. 126 (2004) 5515–5522.

[27] P. Lindqvist-Reis, R. Klenze, G. Schubert, T. Fanghänel, J. Phys. Chem. B 109 (2005) 3077–3083.

[28] T. Vercouter, P. Vitorge, B. Amekraz, E. Giffaut, S. Hubert, C. Moulin, Inorg. Chem. 44 (2005) 5833–5843.

[29] L. Rao, G. Tian, Inorg. Chem. 48 (2009) 964–970.

[30] K. Miyakawa, Y. Kaizu, H. Kobayashi, J. Chem. Soc., Faraday Trans. 1 84 (1988) 1517–1529.

[31] G. Laurenczy, A. E. Merbach, Helv. Chim. Acta 71 (1988) 1971–1973.

[32] P. Lindqvist-Reis, C. Walther, R. Klenze, A. Eichhofer, T. Fanghanel, J. Phys. Chem. B 110 (2006) 5279–5285.

[33] B. T. Thole, Chem. Phys. 59 (1981) 341–350.

[34] M. Souaille, H. Loirat, D. Borgis, M. P. Gaigeot, Comput. Phys. Commun. 180 (2009) 276–301.

[35] W. Wagner, A. Pruss, J. Phys. Chem. Ref. Data 31 (2002) 387–535.

[36] P. P. Ewald, Ann. Phys. 369 (1921) 253–287.

[37] T. S. Hofer, H. T. Tran, C. F. Schwenk, B. M. Rode, J. Comput. Chem. 25 (2004) 211–217.

[38] T. Seward, C. Henderson, J. Charnock, T. Driesner, Geochim. Cosmochim. Acta 63 (1999) 2409–2418.

[39] T. Seward, C. Henderson, J. Charnock, B. Dobson, Geochim. Cosmochim. Acta 60 (1996) 2273–2282.

[40] J. L. Fulton, D. M. Pfund, S. L. Wallen, M. Newville, E. A. Stern, Y. Ma, J. Chem. Phys. 105 (1996) 2161.

[41] D. Hagberg, E. Bednarz, N. M. Edelstein, L. Gagliardi, J. Am. Chem. Soc. 129 (2007) 14136–14137.

Table 1: Hydration properties of Ln^{3+} in aqueous solution as a function of the temperature.

[a] First ($r^{(1)}_{Ln-O}$) and second ($r^{(2)}_{Ln-O}$) peak maximum of Ln-O radial distribution functions (in Å).

[b] Coordination number of the first ($CN^{(1)}$) and the second ($CN^{(2)}$) hydration shell obtained from integration of the first and second radial distribution function's peaks.

[c] Peaks of the O-Ln-O angular distribution functions (in degrees).

[d] Mean Residence Times of water molecules in the first ($MRT^{(1)}$) and the second ($MRT^{(2)}$) hydration shell (in ps).

Ln	T (K)	$r^{(1)a}_{Ln-O}$	$CN^{(1)b}$	θ^{c}_{O-Ln-O}	$MRT^{(1)d}$	$r^{(2)a}_{Ln-O}$	$CN^{(2)b}$	$MRT^{(2)d}$
Nd^{3+}	275	2.48	9.00	70;137	1631	4.63	19.5	9
	302	2.48	9.00	70;137	1482	4.63	19.2	6
	416	2.48	8.99	70;137	261	4.63	18.0	4
	624	2.48	8.93	70;136	39	4.67	14.7	3
Eu^{3+}	277	2.41	8.90	70;137	400	4.58	19.3	9
	290	2.41	8.90	70;137	245	4.58	19.0	8
	422	2.41	8.77	71;137	73	4.58	17.9	4
	614	2.39	8.57	71;138	31	4.60	15.1	3
Gd^{3+}	275	2.39	8.65	71;138	305	4.56	19.1	9
	290	2.39	8.72	71;138	254	4.55	18.9	8
	415	2.39	8.72	71;138	75	4.57	18.9	5
	623	2.38	8.50	72;139	31	4.59	17.4	4
Tb^{3+}	276	2.37	8.48	72;140	249	4.55	19.1	10
	304	2.37	8.59	72;139	171	4.55	18.9	7
	422	2.37	8.57	72;139	69	4.56	19.0	5
	619	2.37	8.42	72;138	33	4.58	17.0	4
Ho^{3+}	283	2.34	8.17	73;119;142	349	4.52	18.8	10
	302	2.34	8.24	73;119;141	246	4.52	18.6	8
	419	2.34	8.36	72; - ;140	78	4.53	17.6	4
	626	2.34	8.26	72; - ;139	34	4.55	14.8	3
Lu^{3+}	276	2.32	8.01	74;118;143	1715	4.50	18.3	11
	293	2.32	8.01	74;118;143	1327	4.50	18.3	10
	415	2.32	8.05	73;121;142	149	4.50	18.1	5
	619	2.32	8.07	73; - ;141	33	4.50	16.6	3

Table 2: Population ratio of the first hydration number CN of different atoms.

[a] Previous study from Ref. [25].

M^{3+}	T (K)	CN = 7	CN = 8	CN = 9	CN = 10	CN = 11
$La^{3+,(a)}$	277	0 %	<1 %	100 %	<1 %	0 %
	299	0 %	0 %	99 %	1 %	0 %
	410	0 %	<1 %	93 %	7 %	0 %
	624	0 %	3 %	84 %	13 %	<1 %
Nd^{3+}	275	0 %	<1 %	100 %	<1 %	0 %
	302	0 %	<1 %	100 %	<1 %	0 %
	416	0 %	1 %	98 %	1 %	0 %
	624	<1 %	10 %	87 %	3 %	0 %
Eu^{3+}	277	0 %	10 %	90 %	<1 %	0 %
	290	0 %	10 %	90 %	0 %	0 %
	422	0 %	23 %	77 %	<1 %	0 %
	614	<1 %	44 %	56 %	<1 %	0 %
Gd^{3+}	275	0 %	35 %	65 %	0 %	0 %
	290	0 %	28 %	72 %	0 %	0 %
	415	<1 %	28 %	72 %	<1 %	0 %
	623	<1 %	50 %	50 %	<1 %	0 %
Tb^{3+}	276	0 %	52 %	48 %	0 %	0 %
	304	0 %	41 %	59 %	0 %	0 %
	422	0 %	43 %	57 %	<1 %	0 %
	619	<1 %	57 %	43 %	<1 %	0 %
Ho^{3+}	283	0 %	83 %	17 %	0 %	0 %
	302	0 %	76 %	24 %	0 %	0 %
	419	<1 %	64 %	36 %	<1 %	0 %
	626	1 %	73 %	26 %	<1 %	0 %
Lu^{3+}	276	<1 %	99 %	1 %	0 %	0 %
	293	0 %	99 %	1 %	0 %	0 %
	415	<1 %	94 %	6 %	0 %	0 %
	619	2 %	89 %	9 %	0 %	0 %

Table 3: Energies changes for Reaction $M(H_2O)_8^{3+} + H_2O \rightleftharpoons M(H_2O)_9^{3+} \times$ (kJ mol^{-1}).

[a] Previous study from Ref. [25].

[b] Experimental study from Ref. [31].

[c] Electrostatic model from Ref. [30].

[d] TRLFS from Ref. [27].

attention le log(k) est bien le log a base 10. Le probleme c'est que pour les anglo-saxons log = ln.

M^{3+}	$\Delta_r H^0_{9,298}$	-298·$\Delta_r S^0_{9,298}$	$\Delta_r G^0_{9,298}$	$\log(K_{9,298})$	E_a
$La^{3+(a)}$	-26.2 ± 2.8	+3.9 ± 2.3	-22.3 ± 3.6	+3.9 ± 0.6	15.2 ± 0.4
Nd^{3+}	-19.5 ± 1.5	+3.5 ± 1.3	-16.1 ± 1.9	+2.8 ± 0.3	15.7 ± 1.7
Eu^{3+}	-8.3 ± 0.8	+3.1 ± 0.7	-5.2 ± 1.0	+0.9 ± 0.2	10.3 ± 0.8
Gd^{3+}	-2.6 ± 2.1	+0.6 ± 1.8	-2.0 ± 2.8	+0.3 ± 0.5	9.4 ± 0.1
Tb^{3+}	-1.2 ± 1.8	+0.8 ± 1.5	-0.4 ± 2.4	+0.1 ± 0.4	8.3 ± 0.1
Ho^{3+}	+2.4 ± 2.0	+0.7 ± 1.7	+3.1 ± 2.6	-0.6 ± 0.5	10.0 ± 0.4
Lu^{3+}	+11.6 ± 1.6	-0.3 ± 1.4	+11.3 ± 2.1	-2.0 ± 0.4	16.8 ± 0.8
$Ce^{3+(b)}$	-13.0	+9.83	-3.17	+0.68	
$Ce^{3+(c)}$	-15	+10	-5	+0.88	
$Cm^{3+(d)}$	-13.1 ± 0.4	+7.6 ± 0.4	-5.5 ± 0.4	+0.96	

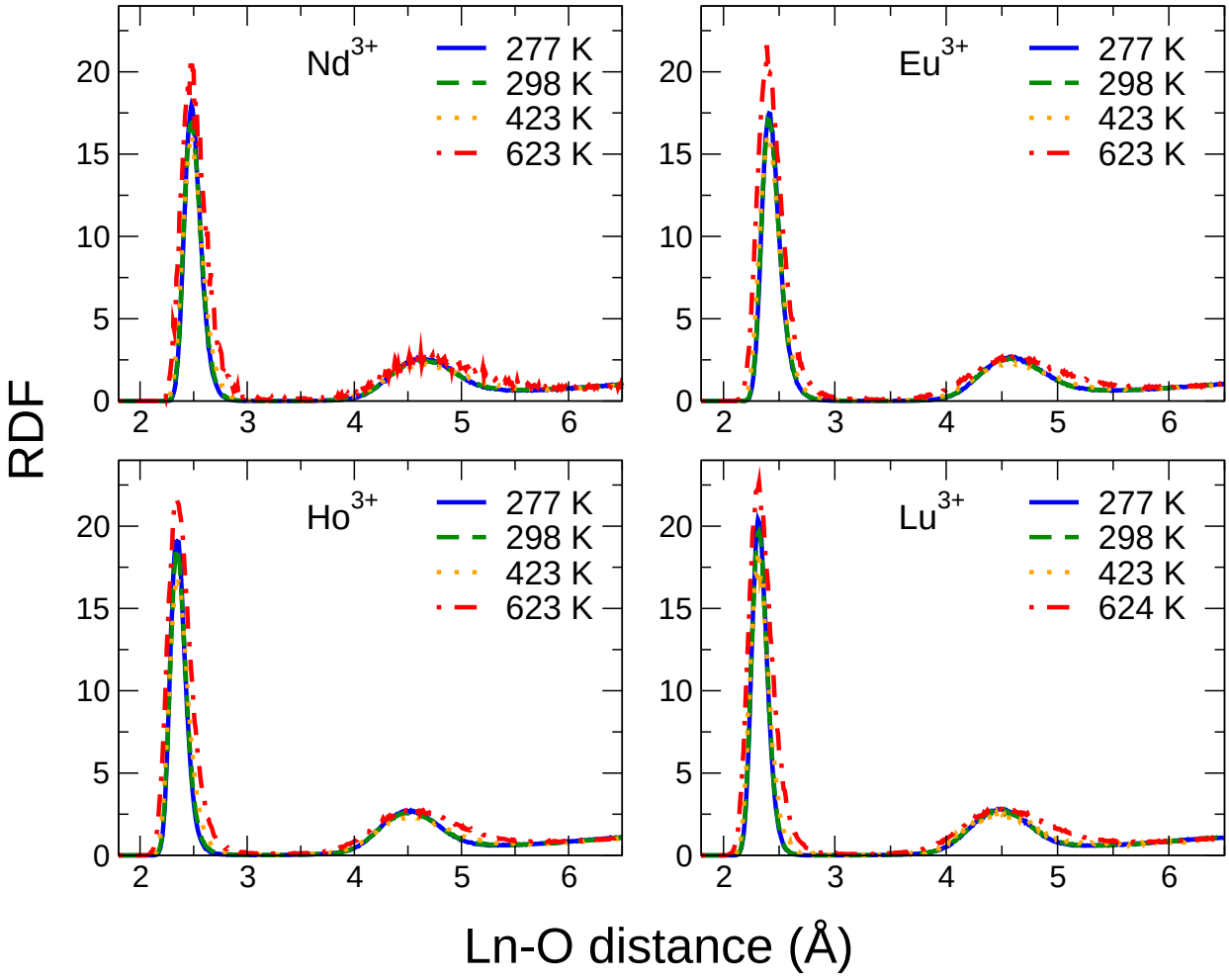

Figure 1: Ln-O radial distribution functions at 277 K (solid line), 298 K (dashed line), 423 K (points) and 623 K (dashed-point line) obtained for Nd^{3+}, Eu^{3+}, Ho^{3+}, and Lu^{3+}.

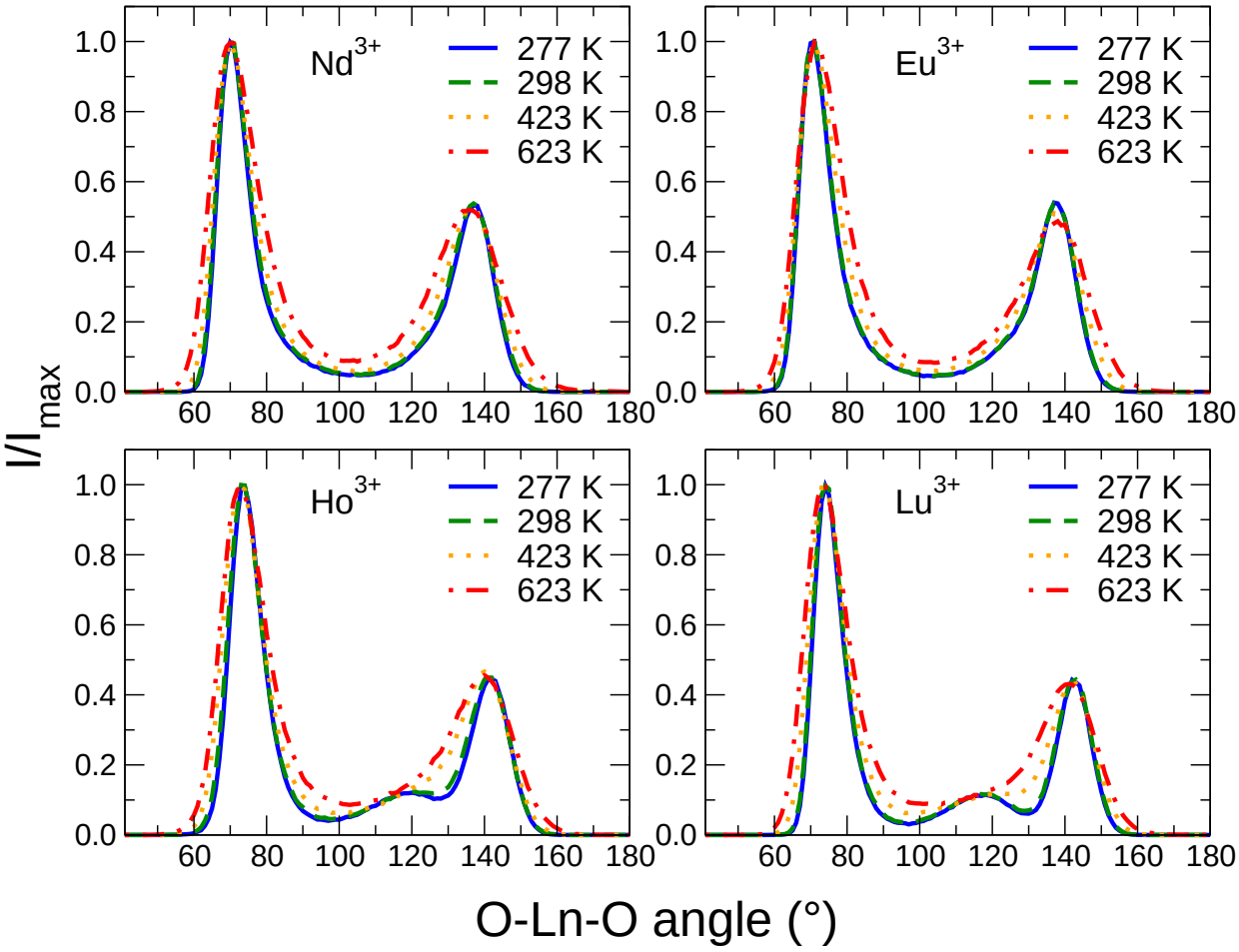

Figure 2: O-Ln-O angular distribution functions of the first hydration shell at 277 K (solid line), 298 K (dashed line), 423 K (points) and 623 K (dashed-point line) obtained for Nd^{3+}, Eu^{3+}, Ho^{3+}, and Lu^{3+}.

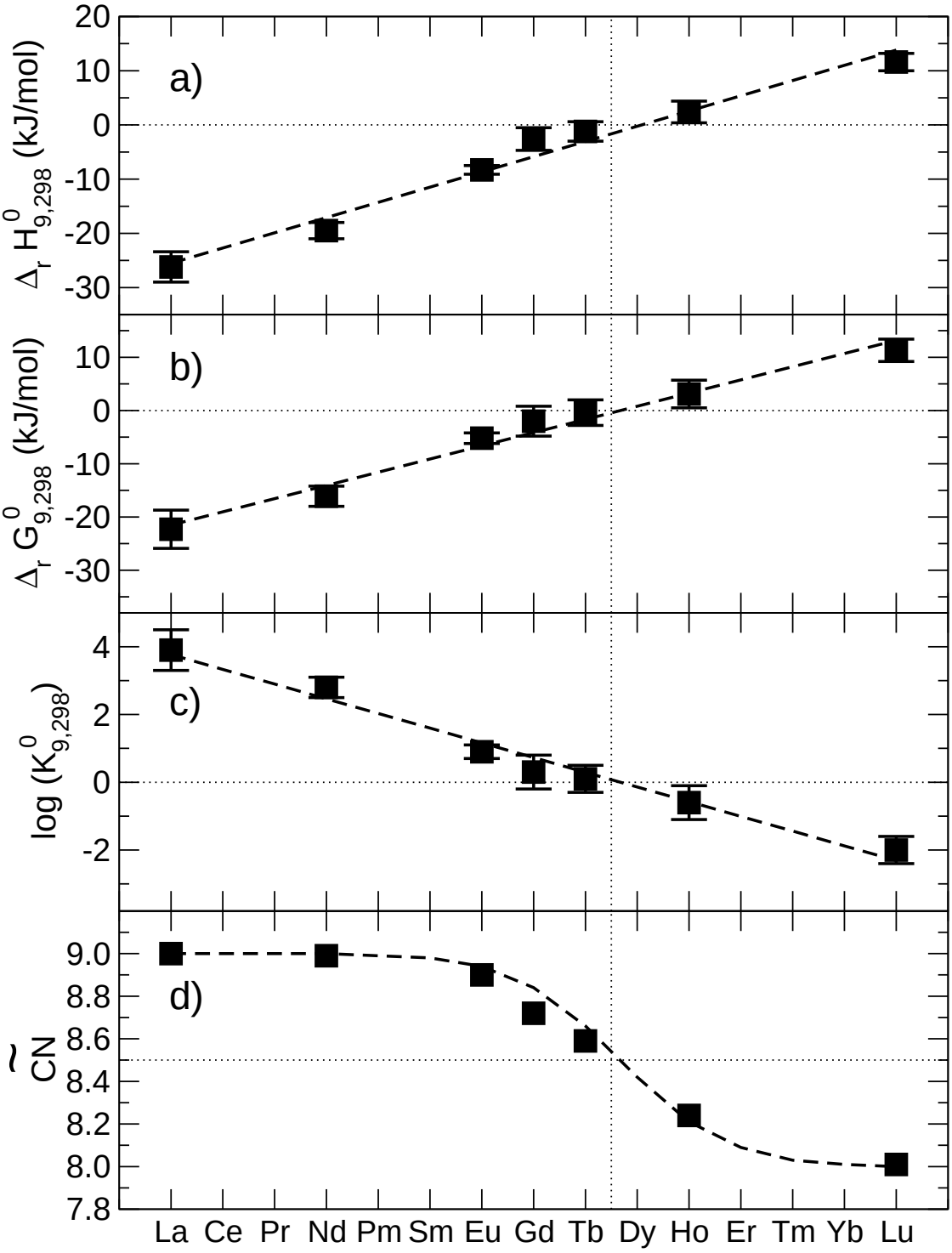

Figure 3: Variations of the thermodynamics parameters for the water exchange reaction (Eq. 1) through the lanthanoid series: a) $\Delta_r H^0_{9,298}$, b) $\Delta_r G^0_{9,298}$, c) $\log(K^0_{9,298})$ and d) $\widetilde{CN}$ obtained as defined in equation 6. Dashed lines on a), b) and c) panels represent the linear regressions and for panel d) is the corresponding curve using equation 7.

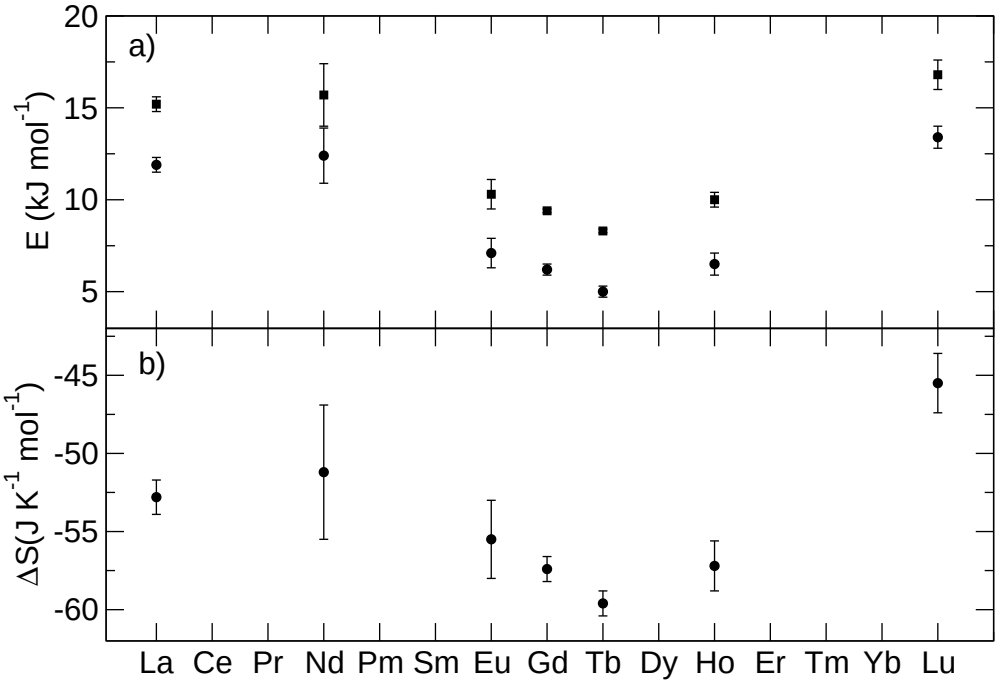

Figure 4: Variation of the activation energy for water self-exchange reaction (Eq. 1), panel a) in squares, of the activation enthalpy, panel a), and entropy, panel b, in circles, through the lanthanoid series.